Low Index Photonic Membrane Textile for Personal Thermoregulation

Salim Assaf, Yan Pennec, Alexander Korovin, Anthony Treizebre, Vincent Thomy, Bahram Djafari-Rouhani

IEMN Université de Lille

Villeneuve d'Ascq, France

E-mail: Salim.Assaf@univ-lille1.fr; yan.pennec@univ-lille1.fr; alexander.korovin@iemn.univ-lille1.fr; Anthony.Treizebre@univ-lille1.fr; Vincent.Thomy@iemn.univ-lille1.fr; Bahram.Djafari-Rouhani@univ-lille1.fr

Abstract— **The effect of a photonic polymer membrane in the Mid InfraRed (MIR) range for passive personal heating regulation is demonstrated. We show that, by designing the holes' diameters and periods of the membrane, we are able to reflect up to 17% of the emission of the human body in the wavelength range [7.5, 11.5] µm. The work presented here has been performed theoretically with the help of the Finite Element Method. The origin of the reflectivity comes from guided and resonant modes belonging to the excitation of the photonic membrane. Integrated to a textile, such a membrane can greatly mitigate the energy demand for indoor heating and ultimately contributes to the relief of the climate issues.**

Keywords- photonic polymer membrane; personal heating regulation; human body; MIR; textile; reflectivity; numerical calculations; Finite Element Method.

I. INTRODUCTION

A large part of the building energy consumption is attributed to temperature control using Heating, Ventilation and Air Conditioning (HVAC) systems [1]. A decrease in this consumption, even slightly, will contribute to both environmental protection and costs saving. One way is to support building insulation; another way is to control the energy consumption by personal thermoregulation [2]. Toward this end, personal thermoregulation properties have been recently developed, not only in extreme environments for military personnel, athletes or emergency medical service personnel [3], but for the majority of people who spend their time in a sedentary state. The personal thermal management has been defined through different devices, wearable like normal clothes, but capable to control the body comfort. Personal cooling textile have been developed using synthetic polymer fibers with low IR absorbance [4][5] or able to enhance the radiative dissipation by nanoporous polyethylene film [6]. The opposite effect, i.e. personal heating textiles, have also been studied. In this case, the personal thermal management has been controlled by the integration of metallic nanowires embedded in the textile that reduce the energy waste from the human body. Such textiles not only reflect the human body infrared radiation, but also allow Joule heating to complement the passive insulation [7]-[9]. Realizing heating and cooling properties within a same structure and without any energy input still remains a tremendous challenge. Very recently, Hsu et al. [10] investigated a dual-mode textile for human body radiative heating using a bilayer thermal emitter embedded inside an IR-transparent nanoPE that can perform both passive radiative heating and cooling using the same piece of textile. A reversible humidity sensitive clothing for personal thermoregulation was also proposed using shape memory polymer [11]. The smart textile has been designed to reversibly adapt the thermal insulation functionality, thus permitting the air flow and reducing the humidity level and the apparent temperature. Therefore, a tremendous effort is necessary to develop smart wearable thermoregulating textiles which can reversibly respond to the immediate temperature feeling of the wearer.

Photonic crystals, proposed in 1987 by Eli Yablonovitch [12] are periodic structures based on patterns whose dimensions are close to the working wavelength. The control and manipulation of waves in photonic crystals are achieved by the generation of band gaps in the Bragg regime for in plane waves. Photonic crystal slabs can also interact with external radiations in complex and interesting ways. Of particular importance here is the presence of resonances within the plate which present a high confined electromagnetic field [13]-[15]. Such interaction is usually presented as Fano phenomenon that occurs when a discrete localized state becomes coupled to a continuum of states [16]. The resonances of the plate can then couple to external radiation and provide an efficient way to channel light from within the slab to the external environment. In addition, the resonances can significantly affect the transmission and reflection of externally incident light, resulting in complex resonant line shapes that are useful in filter applications [17]. Very recently, such property was introduced in topics related to plasmonic [18], electromagnetic metamaterial [19][20], and for different optomechanic [21] or sensing [22][23] applications.

We investigate here the properties of a photonic crystal membrane, tailored in the MIR range, useful for personal heating regulation. The BCB (Benzocyclobutene) is the polymer which compose the photonic membrane. The objective is to increase the reflectance in the MIR range, playing with the geometrical parameters of the membrane. We first describe the photonic polymer membrane under consideration and its physical and geometrical parameters. Then, we show the calculation of the reflective spectrum and study its behavior as a function of the geometrical parameters. The rest of the paper is structured as follows. After this introduction, we describe in Section 2 the design and detail the simulation of the photonic membrane. Then, we conclude the paper in Section 3.

II. DESIGN AND SIMULATION OF A PHOTONIC POLYMER MEMBRANE

As seen schematically Figure 1a, the human body electromagnetic wave is launched from the top and interacts with the photonic membrane. The photonic membrane, embedded in air, is made of a polymer (BCB) and drilled following a triangular array of holes (Figure 1b). We took into consideration the absorption of the BCB by using its complex refractive index. The geometrical parameters involved in the study are the lattice parameter P, the hole's diameter D and the thickness of the membrane h. All numerical results have been performed with the help of the Finite Element Method (FEM) for which the elementary unit cell for the calculation of the transmission, reflection and absorption spectra are sketched Figure 1b. At each side of the unit cell, perfect matching layers (PML) are applied to absorb all outgoing waves while on the plane of the membrane periodic boundary conditions are used to build the infinite periodic membrane.
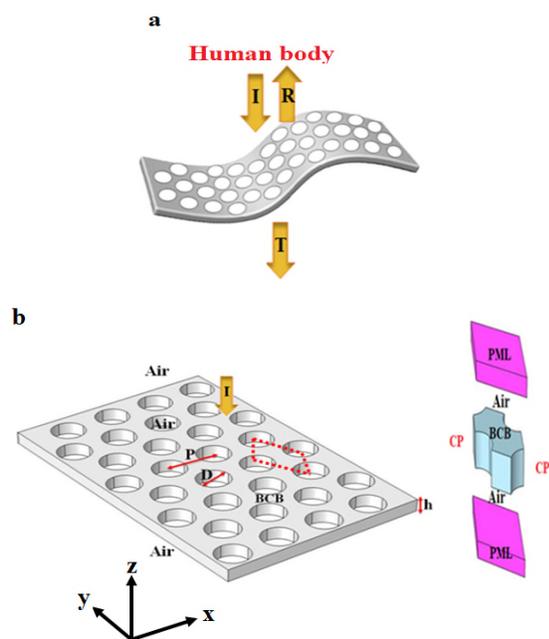
Figure 1. a) Principal scheme of the system with the direction of the incident (I), reflective (R) and transmitive (T) electromagnetic waves. b) (left) 3D view of the BCB membrane where h is the thickness, D the diameter and P the period. (Right) Elementary unit cell used for the FEM calculation with the absorbing (PML) and periodic (CP) boundary conditions.

Figure 2a presents, as a reference, the behavior of a not structured BCB membrane of thickness 4µm, and records the reflection, transmission and absorption curves, reported respectively in black, blue and red. One can see that almost 80% of the signal emitted is transmitted through the membrane. At the wavelengths close to 8 µm, 9.5 µm and 12µm, several dips appear in the transmission curve which correspond to absorption peaks inside the membrane. A small amplitude of reflection (lower than 20%) appears in

the reflection spectrum with a zero reflection at 6µm. This variation is due to the Fabry Perot oscillations inside the BCB membrane of finite thickness. We now structure the membrane, considering a triangular array of holes with the geometrical parameters $P = 7$ µm, $D = 5.5$ µm, and h = 4 µm and record, as before, the reflection (black), transmission (blue) and absorption (red) coefficients (Figure 2b). We find that the spectrum is drastically affected in the wavelength range [6, 7.5] µm. To get a deeper insight, the reflection coefficient is magnified in the inset of Figure 2b. One can see that the reflection comes from the existence of two main peaks and a small one in the middle. To understand their origin, we perform the calculation of the distribution of the electric field in the unit cell at the wavelengths 6.08 µm, 6.41 µm and 6.88 µm corresponding respectively to the three features (Figure 2c). The two high reflection peaks come from the excitation of the guided modes, which spread over the BCB membrane. One is antisymmetric while the other is symmetric with respect to the middle plane of the membrane. The small peak in the middle corresponds to an antisymmetric mode strongly confined inside the air hole. One can note that this localized mode, in interaction with the emitted continuum, gives rise to a peak of asymmetric shape in the reflection spectrum. Such physical properties are known as a Fano resonance [15].
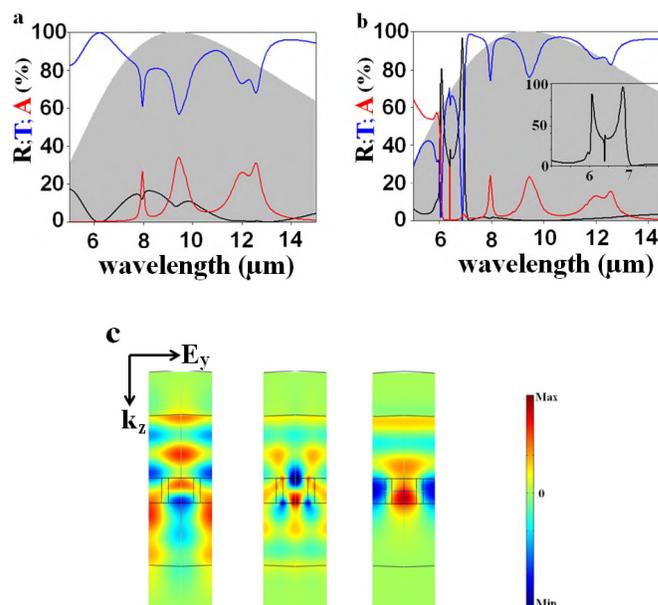
Figure 2. a) Reflection (black), transmission (blue) and absorption (red) coefficients through a) the non-structured membrane with h = 4 µm and b) the structured membrane with P = 7 µm, D = 5.5 µm, and h = 4 µm. The grey hatched area represents the emissivity of the human body at 37°C. c) Representation of the electric field Ey at the wavelengths λ =6.08 µm ; λ = 6.41 µm, and λ = 6.88 µm, corresponding respectively to the three features in the inset of b).

Figures 2a and 2b show the emissivity of the human body at 37°C calculated from the Planck law and represented with the grey hatched area. One can see that, with the chosen set of geometrical parameters, the reflection

curve has been affected in the lower part of the emissive spectrum. In Figure 3a, the geometrical parameters of the photonic structure have been changed with P = 9 μm and D = 6.5 μm. One can see that the peaks of reflection shift to the higher wavelength and now reach the area where the maximum of the emissive spectrum is expected. It remains that the shape of the signal is the same, composed of two main peaks and the Fano shape resonance in between. Nevertheless, the amplitude has decreased, due to the presence of the polymer absorption which was not present in the previous case.

We then demonstrated that the resonant modes of the low index polymer membrane can be used to produce a reflection in the MIR range. To get a quantitative representation of the global reflection as a function of the geometrical parameters, we define an efficiency coefficient, η, which corresponds to a numerical integration of the reflection over a wavelength range under consideration, normalized with respect to the emissivity of the human body. So, all the efficiency factors should be comprised between 0 and 1, with a maximum of reflection when $\eta = 1$. This factor is explained through the following formula:

$$\eta = \frac{\int_{\lambda_{min}}^{\lambda_{max}} E_\lambda . R_\lambda . d\lambda}{\int_{\lambda_{min}}^{\lambda_{max}} E_\lambda} \quad (1)$$

where E_λ is the human body emissivity at the wavelength λ and R_λ is the structure's reflectance over the wavelength range [λ_{min} = 7.5 μm, λ_{max} = 11.5 μm].
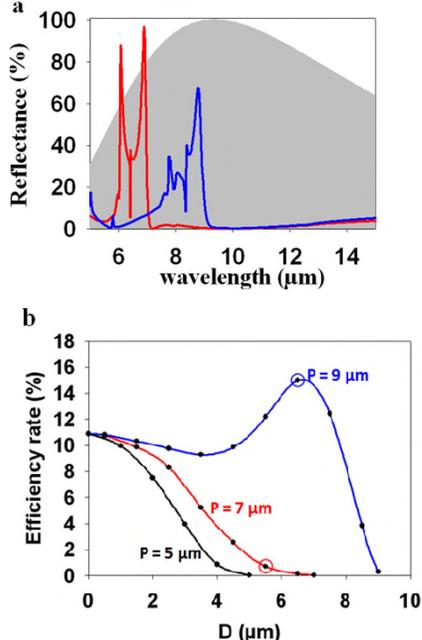
Figure 3. a) Reflection spectra for: P = 7 μm and D = 5.5 μm (red curve) and P = 9 μm and D = 6.5 μm (blue curve) with h = 4 μm b) Evolution of the efficient rate η as a function of D, for three periods P (h = 4 μm). The circled dots correspond to the position of the two reflection spectra in a).
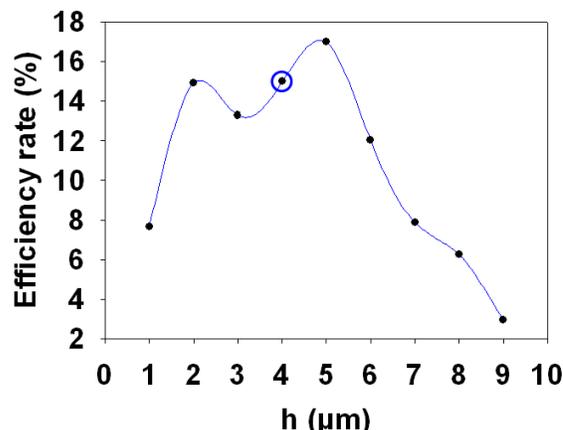
Figure 4. Evolution of the efficiency reflection coefficient η as a function of h, with P = 9 μm and D = 6.5 μm. The circled dot corresponds to the position of the blue reflection spectrum in a).

Figure 3 shows the evolution of the efficiency coefficient (in %) as a function of the diameter of the holes, for different periods and for a constant thickness of the membrane, $h = 4$ μm. One can see that η clearly depends of the geometrical parameters and a maximum of reflectance (~15 %) is reached for a period $P = 9$ μm and a diameter $D = 7$ μm. The origin of the variation of η comes from the shift of the two peaks described in the previous section through the wavelength range [7.5, 11.5] μm, which presents the higher level of emissivity of the human body. Figure 4 represents the behavior of the efficiency coefficient as a function of the thickness of the membrane. The circled blue dot in the curve corresponds to the maximum of the efficiency obtained from Figure 3 corresponding to the geometrical parameters P = 9 μm, D= 6.5 μm and h = 4 μm. One can see that the response of the efficiency coefficient is robust with respect to the thickness variation of the membrane and even more the efficiency can still be increased, reaching 17% of reflectivity.

III.   CONCLUSION

The effect of reflectance of a photonic membrane of low refractive index on the human body emission at 37°C has been theoretically investigated in the MIR range. We showed that the reflectivity depends on the geometrical parameters of the membrane and found the occurrence of three peaks of reflection whose origin is due to the structuring of the membrane. One origin is due to the photonic guided modes inside the membrane, the second one comes from the local excitation of the electromagnetic field inside the air holes. The dependence of the geometrical parameters has been quantitatively highlighted through the definition of an efficiency coefficient. We found that the BCB membrane can reflect up to 17% of the emission in the wavelength range [7.5, 11.5] μm which correspond to the maximum of the human body emissivity.

We are currently studying the effect of the physical parameters considering the behavior of the refractive index of both the membrane and the environment on the reflectivity rate. Also, the work is ongoing toward an experimental demonstration. This work paves the way for the design of a smart responsive photonic membrane which dynamically modifies its reflectance in response to external stimuli like temperature or humidity.

REFERENCES

[1] K. J. Chua, S. K. Chou, W. M. Yang, and J. Yan, "Achieving better energy-efficient air conditioning – A review of technologies and strategies," *Appl. Energy*, vol. 104, pp. 87–104, Apr. 2013.

[2] R. F. Rupp, N. G. Vásquez, and R. Lamberts, "A review of human thermal comfort in the built environment," *Energy Build.*, vol. 105, pp. 178–205, Oct. 2015.

[3] M. M. Yazdi and M. Sheikhzadeh, "Personal cooling garments: a review," *J. Text. Inst.*, vol. 105, no. 12, pp. 1231–1250, 2014.

[4] J. K. Tong, X. Huang, S. V. Boriskina, J. Loomis, Y. Xu, and G. Chen, "Infrared-Transparent Visible-Opaque Fabrics for Wearable Personal Thermal Management," *ACS Photonics*, vol. 2, no. 6, pp. 769–778, Jun. 2015.

[5] P. B. Catrysse, A. Y. Song, and S. Fan, "Photonic Structure Textile Design for Localized Thermal Cooling Based on a Fiber Blending Scheme," *ACS Photonics*, vol. 3, no. 12, pp. 2420–2426, Dec. 2016.

[6] P.-C. Hsu *et al.*, "Radiative human body cooling by nanoporous polyethylene textile," *Science*, vol. 353, no. 6303, pp. 1019–1023, Sep. 2016.

[7] P.-C. Hsu *et al.*, "Personal Thermal Management by Metallic Nanowire-Coated Textile," *Nano Lett.*, vol. 15, no. 1, pp. 365–371, Jan. 2015.

[8] Z. Yu, Y. Gao, X. Di, and H. Luo, "Cotton modified with silver-nanowires/polydopamine for a wearable thermal management device," *RSC Adv.*, vol. 6, no. 72, pp. 67771–67777, 2016.

[9] L. Cai *et al.*, "Warming up human body by nanoporous metallized polyethylene textile," *Nat. Commun.*, vol. 8, no. 1, Dec. 2017.

[10] P.-C. Hsu *et al.*, "A dual-mode textile for human body radiative heating and cooling," *Sci. Adv.*, vol. 3, no. 11, p. e1700895, Nov. 2017.

[11] Y. Zhong *et al.*, "Reversible Humidity Sensitive Clothing for Personal Thermoregulation," *Sci. Rep.*, vol. 7, p. 44208, Mar. 2017.

[12] E. Yablonovitch, "Inhibited Spontaneous Emission in Solid-State Physics and Electronics," *Phys. Rev. Lett.*, vol. 58, no. 20, p. 4, 1987.

[13] V. N. Astratov *et al.*, "Resonant coupling of near-infrared radiation to photonic band structure waveguides," *J. Light. Technol.*, vol. 17, no. 11, pp. 2050–2057, Nov. 1999.

[14] V. Pacradouni, W. J. Mandeville, A. R. Cowan, P. Paddon, J. F. Young, and S. R. Johnson, "Photonic band structure of dielectric membranes periodically textured in two dimensions," *Phys. Rev. B*, vol. 62, no. 7, pp. 4204–4207, Aug. 2000.

[15] A. R. Cowan, P. Paddon, V. Pacradouni, and J. F. Young, "Resonant scattering and mode coupling in two-dimensional textured planar waveguides," *J. Opt. Soc. Am. A*, vol. 18, no. 5, p. 1160, May 2001.

[16] M. F. Limonov, M. V. Rybin, A. N. Poddubny, and Y. S. Kivshar, "Fano resonances in photonics," *Nat. Photonics*, vol. 11, no. 9, pp. 543–554, Sep. 2017.

[17] P. Markoš, "Fano resonances and band structure of two-dimensional photonic structures," *Phys. Rev. A*, vol. 92, no. 4, Oct. 2015.

[18] B. Luk'yanchuk *et al.*, "The Fano resonance in plasmonic nanostructures and metamaterials," *Nat. Mater.*, vol. 9, no. 9, pp. 707–715, Sep. 2010.

[19] A. B. Khanikaev, C. Wu, and G. Shvets, "Fano-resonant metamaterials and their applications," *Nanophotonics*, vol. 2, no. 4, Jan. 2013.

[20] Y. Yang, I. I. Kravchenko, D. P. Briggs, and J. Valentine, "All-dielectric metasurface analogue of electromagnetically induced transparency," *Nat. Commun.*, vol. 5, p. 5753, Dec. 2014.

[21] K. A. Yasir and W.-M. Liu, "Controlled Electromagnetically Induced Transparency and Fano Resonances in Hybrid BEC-Optomechanics," *Sci. Rep.*, vol. 6, no. 1, Sep. 2016.

[22] S. Amoudache *et al.*, "Optical and acoustic sensing using Fano-like resonances in dual phononic and photonic crystal plate," *J. Appl. Phys.*, vol. 119, no. 11, p. 114502, Mar. 2016.

[23] N. S. King *et al.*, "Fano Resonant Aluminum Nanoclusters for Plasmonic Colorimetric Sensing," *ACS Nano*, vol. 9, no. 11, pp. 10628–10636, Nov. 2015.